

# State dependence of tunneling processes and nuclear fusion

Roberto Onofrio<sup>1</sup> and Carlo Presilla<sup>2,3</sup>

<sup>1</sup>*Department of Physics and Astronomy, Dartmouth College,  
6127 Wilder Laboratory, Hanover, NH 03755, USA*

<sup>2</sup>*Dipartimento di Matematica, Sapienza Università di Roma, Piazzale Aldo Moro 2, Roma 00185, Italy*

<sup>3</sup>*Istituto Nazionale di Fisica Nucleare, Sezione di Roma 1, Roma 00185, Italy*

We discuss the sensitivity of tunneling processes to the initial preparation of the quantum state. We compare the case of Gaussian wave packets of different positional variances using a generalized Woods-Saxon potential for which analytical expressions of the tunneling coefficients are available. Using realistic parameters for barrier potentials we find that the usual plane wave approximation underestimates fusion reactivities by an order of magnitude in a range of temperatures of practical relevance for controlled energy production.

Tunneling processes are of crucial relevance to a broad range of physical systems, including semiconductors [1] and heterostructures [2],  $\alpha$ -radioactivity and nuclear fusion in stars [3–5], the early Universe [6], and nuclear fusion processes in the laboratory [7–10]. Apart from an early contribution [11], tunneling probabilities have been usually evaluated by considering incoming plane waves. However in realistic settings as the ones mentioned above, the particles undergoing tunneling cannot in general be fully described by plane waves, either because particles are confined in space, or because in a many-body setting they undergo scattering with other particles, thereby limiting the coherence length of the plane wave [12]. Moreover, there are discrepancies between theoretical expectations and data from fusion experiments [13] and therefore it may be important to scrutinize all the underlying theoretical assumptions.

It is therefore important to discuss the robustness of tunneling coefficients and fusion reactivities with respect to the choice of more general initial states, for instance by considering the representative set of Gaussian wave packets. The use of generalized Gaussian wave packets has been already pioneered by Dodonov and collaborators [14–16], with results confirming that the predictions on tunneling rates may differ even orders of magnitude with respect to the one arising from the Wentzel-Kramers-Brillouin (WKB) approximation usually employed for fusion reactivities. These studies, in particular [15], have been focused on analytical expressions valid under specific conditions, not necessarily encompassing the entire parameter space.

The main goal of the present paper is to extend the above results evaluating the tunneling coefficient for arbitrary values of the position and momentum spreading. A key ingredient of our analysis is the discussion of a potential admitting exact solutions for the tunneling coefficient in the entire energy range. This allows us to pinpoint differences arising from the sole structure of the incoming Gaussian wave packets, excluding other sources of differences as the ones due to the use of approximations in the calculating techniques, for instance the WKB method. Additionally, we provide more intuitive argu-

ments for the behavior of the fusion reactivity in both the cases of very narrow and very broad positional variances. Finally, we also caution about using approximations like the WKB or the Hill-Wheeler ones, since estimates of tunneling coefficients may differ various orders of magnitude from their exact evaluation.

We focus the attention on the Generalized Woods-Saxon (GWS) potential energy for a one-dimensional system first introduced in [18] (see also [19] for a simpler treatment)

$$V(x) = -\frac{V_0}{1 + e^{a(|x|-L)}} + \frac{W_0 e^{a(|x|-L)}}{(1 + e^{a(|x|-L)})^2}, \quad (1)$$

where both  $V_0$  and  $W_0$  determine the peak values of the potential energy, and  $L, a$ , as in the usual Woods-Saxon potential, determine, respectively, the size of the effective well around the origin and its spatial spread. For a convenient choice of these four parameters, the GWS potential represents a symmetric well with value in the origin equal to  $-V_0/(1 + \exp(-aL)) + W_0 \exp(-aL)/(1 + \exp(-aL))^2$ , and  $-V_0/2 + W_0/4$  at  $|x| = L$ . At large distances  $|x| \gg L$  the potential energy decreases exponentially to zero as  $V(x) \simeq (W_0 - V_0) \exp(-ax)$ , *i.e.*, within a range  $\lambda \simeq 1/a$ . This means that a semiquantitative difference from potential energies of interest for instance in nuclear fusion is that the barrier experienced by the nucleons, if schematized with this potential, does not have the long range as expected for Coulomb interactions, though in a realistic plasma the latter are screened on the Debye length. We choose the set of parameters as described in the caption of Fig. 1, resulting in well depth, barrier height and width of the well comparable to the ones of light nuclei.

Using this potential and the related solutions in terms of tunneling coefficients  $T(E)$  evaluated for plane waves at energy  $E$ , we have considered more general cases of wave localized in both space and momentum. The most practical case, though not exhaustive of all possibilities, is a Gaussian wavepacket.

Let us consider an initial Gaussian wavepacket with positional variance  $\xi^2$ , wave vector  $K$  and mean energy

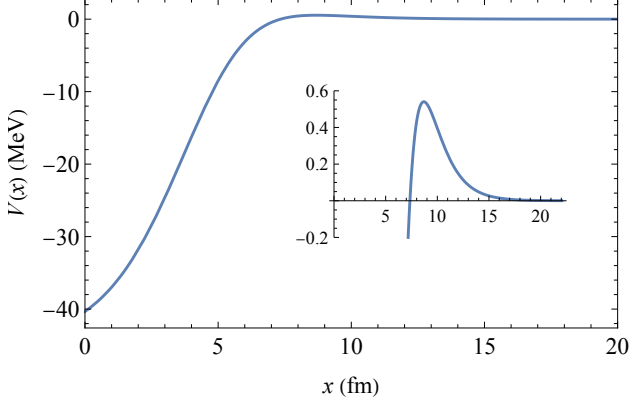


FIG. 1: Positive abscissa plot of the symmetric Generalized Woods-Saxon potential [18] experienced between two nuclei, with parameters  $a = 0.6 \text{ fm}^{-1}$ ,  $L = 5 \text{ fm}$ ,  $V_0 = 45 \text{ MeV}$ , and  $W_0 = 56 \text{ MeV}$ . With these parameters the barrier height (from zero to the maximum positive value of  $V(x)$ ) is  $0.540 \text{ MeV}$ , the well width and depth are  $7.35 \text{ fm}$  and  $40.336 \text{ MeV}$ , respectively. All following figures are obtained using these parameters. The inset (vertical units in MeV, horizontal units in fm) allows to better identify the shape of the barrier otherwise barely visible on the broader scale of the well depth.

$\hbar^2 K^2/(2m)$ :

$$\psi(x, 0) = \left( \frac{2}{\pi \xi^2} \right)^{1/4} e^{-(x-x_0)^2/\xi^2 + iKx}. \quad (2)$$

The corresponding wavefunction in wave vector space  $k$  is

$$\begin{aligned} \varphi(k) &= \frac{1}{\sqrt{2\pi}} \int_{-\infty}^{+\infty} \psi(x, 0) e^{-ikx} dx \\ &= \frac{1}{(2\pi)^{1/4}} \sqrt{\xi} e^{-\xi^2(k-K)^2/4} e^{i(K-k)x}. \end{aligned} \quad (3)$$

Then the probability density for a given wave vector  $k$  is a Gaussian function of  $k$

$$P(k, K) = |\varphi(k)|^2 = \frac{\xi}{\sqrt{2\pi}} e^{-\xi^2(k-K)^2/2}, \quad (4)$$

where we have introduced the positional spreading  $\xi$  as the square root of the positional variance. The probability density  $P(k, K)$  represents a function of  $k$  peaked, for a symmetric distribution, at the average wave vector  $K$ .

We now assume that the wave vector  $K$  belongs to a statistical distribution determined by a one-dimensional Maxwell-Boltzmann distribution with inverse temperature  $\beta$ , namely,

$$w(K, \beta)_{MB} = \left( \frac{\beta \hbar^2}{\pi 2m} \right)^{1/2} e^{-\beta \hbar^2 K^2/(2m)}. \quad (5)$$

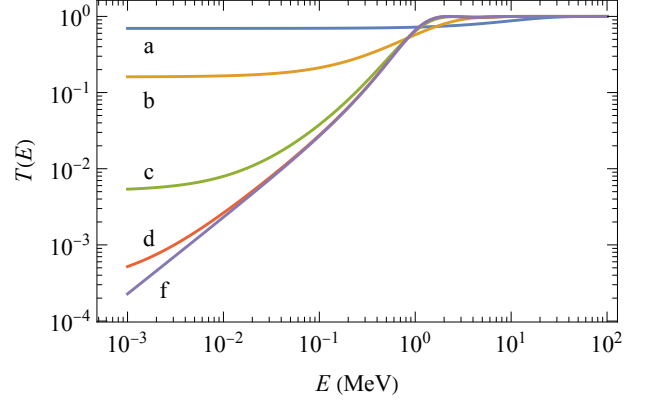


FIG. 2: Transmission coefficient of a Gaussian wave packet of width  $\xi$  and average energy  $E$  impinging on the GWS potential of Fig. 1. Curves from a to d respectively correspond to the cases  $\xi = 2, 8, 32, 128 \text{ fm}$ , while the case of tunneling of a plane wave f is also depicted, clearly showing resonant tunneling oscillations, also noticeable for the larger and finite  $\xi$  values in c and d.

with  $m = m_a m_b / (m_a + m_b)$  the reduced mass of the two interacting nuclei  $a$  and  $b$ .

Particularly relevant is the reactivity defined as  $\langle \sigma(E) v(E) \rangle_{MB}$  where  $\langle \dots \rangle_{MB}$  denotes the statistical average, in our case over the Maxwell-Boltzmann distribution (5),  $\sigma$  is the cross-section of a generic process, and  $v$  is the particle velocity. In the case of fusion, the cross-section is defined as

$$\sigma(E) = \frac{\pi}{k^2} T(E) = \frac{\pi \hbar^2}{\sqrt{2m^3}} \frac{1}{\sqrt{E}} T(E), \quad (6)$$

with the energy  $E = \hbar^2 k^2 / 2m$ .

When referred to the wave vector decomposition, the fusion reactivity is written as:

$$\begin{aligned} \langle \sigma v \rangle_{MB} &= \frac{\pi \hbar^2}{\sqrt{2m^3}} \int_{-\infty}^{+\infty} dk \int_{-\infty}^{+\infty} dK \left( \frac{\hbar^2 k^2}{2m} \right)^{-1/2} \\ &\quad \times T\left( \frac{\hbar^2 k^2}{2m} \right) P(k, K) w(K, \beta)_{MB}. \end{aligned} \quad (7)$$

The integral over  $K$  can be evaluated analytically in the case of Gaussian wavepackets, yielding the rather compact formula

$$\langle \sigma v \rangle_{MB} = \frac{\sqrt{\pi} \hbar}{2} \frac{1}{m} \int_{-\infty}^{+\infty} dk \frac{1}{k} T\left( \frac{\hbar^2 k^2}{2m} \right) \xi_{\text{eff}} e^{-\xi_{\text{eff}}^2 k^2/2}, \quad (8)$$

where we have introduced an effective positional spreading  $\xi_{\text{eff}}$ , depending on the inverse temperature, such that

$$\frac{1}{\xi_{\text{eff}}^2} = \frac{1}{\xi^2} + \frac{m}{\beta \hbar^2}. \quad (9)$$

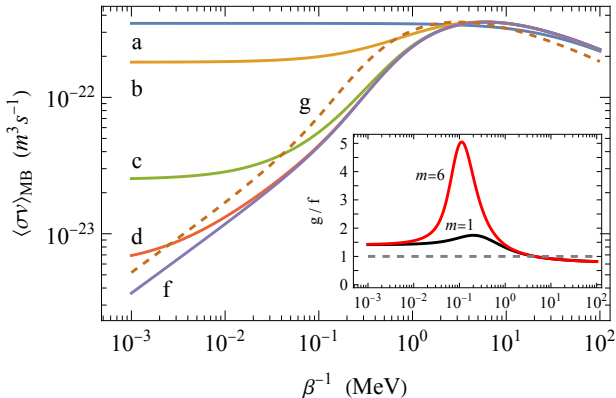


FIG. 3: Fusion reactivity, evaluated for the same Gaussian wave packets of Fig. 2 (and same labeling a-f) with energy  $E$  averaged over a Maxwell-Boltzmann distribution as a function of the temperature  $\beta^{-1}$ . The dashed line (case g) is the case in which the positional spreading depends on temperature as  $\xi = \lambda(\beta)/\sqrt{2}$ , where  $\lambda(\beta)$  is the thermal wavelength of the nuclei [20]. The ratio between this latter curve and the curve for a plain wave (case f) versus  $\beta^{-1}$  is reported in the inset to evidence their differences in a region of interest for nuclear fusion.

For states approximating a plane wave  $\xi^2 \gg \beta\hbar^2/m$ , therefore  $\xi_{\text{eff}}^2 \simeq \beta\hbar^2/m$ , i.e.,  $\xi_{\text{eff}}$  becomes the thermal De Broglie wavelength. In the opposite limit of states highly localized in position,  $\xi^2 \ll \beta\hbar^2/m$ , we have  $\xi_{\text{eff}} \simeq \xi$ . This shows that even assuming an initial quantum state with positional variance of quantum nature, at temperature large enough the relevant lengthscale below which quantum coherence of the wavepacket is maintained no longer depends on the initial preparation. Analogous conclusions have been already obtained in [20, 21]. This can also be interpreted, in the case of a gas at given temperature and density, as corresponding to the mean free path in between two thermal collisions between two particles.

The tunneling coefficient versus the average energy of the wave packet  $E$  is depicted in Fig. 2 for various values of the width of the Gaussian wave packet  $\xi$ . The dependence of the tunneling coefficient on  $E$  is, quite predictably, mild when the value of  $E$  is comparable or higher than the barrier height. Instead its dependence at lower energies strongly depends on  $\xi$ , with the case of plane waves (in the limit of  $\xi \rightarrow +\infty$ ) underestimating the transmission coefficient by even five orders of magnitude at the lowest reported energies, with respect to the case of a Gaussian wave packet with size  $\xi$  smaller than the size of the effective well. The case of small positional variance should correspond, for a state of minimal quantum uncertainty, to a broad distribution of possible momenta, including some corresponding to kinetic energies comparable or higher than the barrier height. Notice the presence of resonant tunneling in the case of plane waves

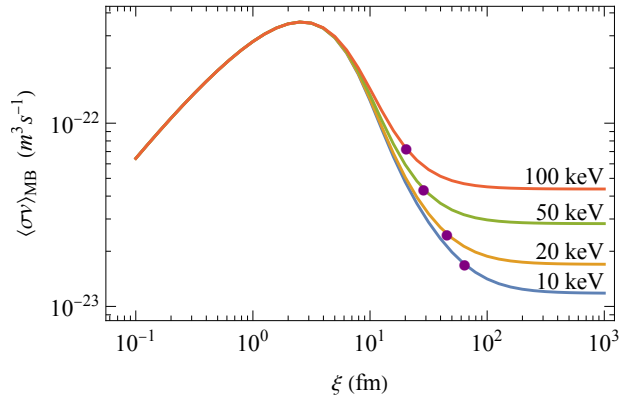


FIG. 4: Fusion reactivity versus the positional spreading  $\xi$  for four temperature values  $\beta^{-1} = 10, 20, 50, 100$  keV of relevance in fusion of light nuclei. The dots denote the reactivities for the positional spreading from the thermal wavelength of the nuclei as discussed in Fig. 3 and evaluated at the corresponding temperatures shown here.

and spatially delocalized Gaussian wave packets, which is instead washed out in the integration when considering Gaussian wave packets of smaller width in position, and therefore broader in momentum/wave vector space.

In Fig. 3 we present the reactivity corresponding to a Maxwell-Boltzmann distribution versus temperature for different values of the positional spreading  $\xi$ . Reflecting the results presented in Fig. 2, the high temperature behavior is the same for the various cases, while at low temperature the same pattern appears, with the highest reactivity occurring for the Gaussian wavepacket of smallest value. Notice a further curve (dashed) which is evaluated for a temperature-dependent positional spreading as discussed in [20]. This curve is relevant for at least two reasons. First, without any active control of the positional variance of the wavepacket, this is what we expect by considering a gas of reagents with a Maxwell-Boltzmann distribution. Secondly, in the temperature range between 10 keV and 100 keV, of interest for controlled thermonuclear fusion, we estimate a boost of the reactivities if compared to the ones achieved by considering plane waves. This is more easily noticeable in the inset, where we report the ratio between the dashed curve of Fig. 3 and the curve corresponding to the prediction of plane waves, curve f, always versus the temperature. In the above mentioned range the ratio is about 1.5, followed by a mild increase to almost 2, then becoming smaller than unity at even higher temperatures. The peak value of the ratio depends on the involved nucleons, as shown in the comparison of the two nucleons with a mass of 2 a.m.u. (reduced mass of 1 a.m.u.) and 12 a.m.u. (reduced mass of 6 a.m.u.). While the latter example has been chosen having in mind the case of Carbon quite rel-

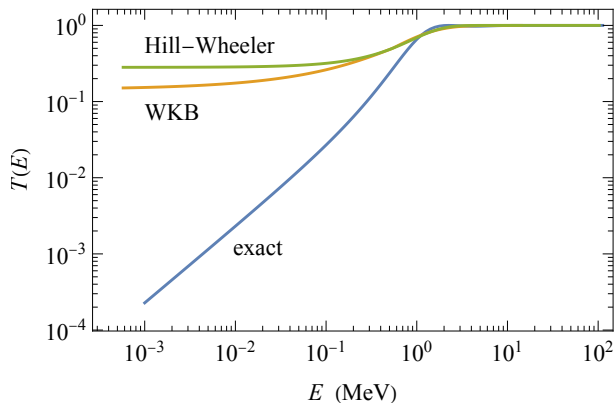


FIG. 5: Transmission coefficient of the same GWS potential as in Fig. 1 for a plane wave versus energy  $E$  evaluated with the exact solution, the WKB approximation, and the Hill-Wheeler approximation.

evant in astrophysics, it should be kept in mind that the same GWS potential is used in both cases to see the sole dependence on the mass, which is unrealistic for Carbon especially in regard to its actual larger well width.

We emphasize more these considerations from a complementary standpoint by plotting the reactivity as a function of the positional variance  $\xi$  for values of temperature relevant to fusion processes of light nuclei,  $\beta^{-1} = 10, 20, 50, 100$  keV, as depicted in Fig. 4. This plot allows to better appreciate that there is an optimal value of  $\xi$  maximizing the reactivity at a given temperature. Indeed, in the case of  $\xi \rightarrow 0$  there will be increasing components of the wave packet at large  $k$ . These components will saturate the transmission coefficient to its maximum value, and will strongly suppress the cross-section due to the dependence of the latter upon  $1/k^2$ , with the overall dependence on reactivity then scaling as the inverse of the wave vector.

The above results have been tested for various choices of the parameters of the potential (it is worth to point out that by construction the GWS potential has a cusp in the origin) with outcome qualitatively similar to the specific case considered in this paper. We expect robustness also in the case of a potential which is the sum of a flat potential at distances smaller than the average radius of the nuclei, and a Coulombian potential. The outcome should also hold in the more realistic three-dimensional setting, when including effects due to the angular momentum term, and a spherically symmetric electric field inside the nucleus assuming uniform electric charge density. However, more extensive analyses will be necessary to determine the quantitative gain in using optimized Gaussian wave packets under these more realistic, yet not susceptible of analytic solutions, situations.

Finally, we discuss the dependence of the tunneling

coefficient upon the adopted calculating scheme, under the hypothesis of plane waves for the tunneling particles. This allows us to contrast the widespread WKB approximation, the Hill-Wheeler approximation, and the exact evaluation of the tunneling coefficient. As noticeable in Fig. 5, both the approximations provide unreliable results with respect to the exact case, in a regime of crucial importance for controlled nuclear fusion, i.e., at energies well below the barrier energy. The discrepancy between the Hill-Wheeler approximation - a further simplification of the WKB method - and the WKB expectation is understandable due to the modelization of the barrier as an inverted parabola, and results in overestimating the tunneling coefficient by about one order of magnitude with respect to the latter. More surprising is the fact that WKB provides tunneling coefficients higher by two orders of magnitude at  $E=10$  keV, and three orders of magnitude at  $E=1$  keV, with respect to the analytical result. This introduces a further element of uncertainty in the estimation of fusion cross-sections if not evaluated from exact solutions or precision numerical evaluations. It should also be remarked that this discrepancy may be quite sensitive to the specific form of the potential energy. In our specific case the absence of a substantial tail for the GWS potential at large distances, instead characteristic of the Coulomb case, could affect the discrepancy among the various cases, creating less sensitivity to the details of the potential at the base of the barrier [23].

In conclusion, we have investigated the sensitivity of tunneling processes to the preparation of Gaussian wave packets - and contrasted to the usually assumed case of plane waves - in the case of an analytically solvable potential, and we have evidenced a relevant sensitivity of the resulting reactivities for fusion processes. It is unclear how to engineer Gaussian states of well-defined, targeted, positional variance. Nevertheless, we have shown that Gaussian states weighted with Maxwell-Boltzmann energy distributions may result in a temperature-dependent positional variance, providing a natural way to enhance fusion reactivities. This is a further stimulus to design thermonuclear fusion prototypes in which emphasis is put in maximizing the plasma temperature with more moderate plasma density, an important point for achieving deuterium-deuterium fusion, with well-known advantages with respect to the currently experimentally investigated deuterium-tritium fusion.

- 
- [1] L. Esaki, New phenomenon in narrow Germanium p-n junctions, *Phys. Rev.* **109**, 603 (1958).
  - [2] F. T. Vasko and A. V. Kuznetsov, Tunneling in Heterostructures. In: *Electronic States and Optical Transitions in Semiconductor Heterostructures*, Graduate Texts in Contemporary Physics. Springer, New York, NY (1999).

- [3] G. Gamow, Zur Quantentheorie der Atomkernes, *Z. Physik* **51**, 204 (1928).
- [4] R. W. Gurney and E. U. Condon, Quantum mechanics and Radioactive Disintegration, *Nature* **122**, 439 (1928); *Phys. Rev.* **33**, 127 (1929).
- [5] E. G. Adelberger, *et al.*, Solar fusion cross-sections, *Rev. Mod. Phys.* **70**, 1265 (1998).
- [6] D. Atkatz and H. Pagels, Origin of the Universe as a quantum tunneling event, *Phys. Rev. D* **25**, 2065 (1982).
- [7] A. B. Balantekin and N. Takigawa, Quantum tunneling in nuclear fusion, *Rev. Mod. Phys.* **70**, 77 (1998).
- [8] R. Vanderbosch, Angular momentum distributions in subbarrier fusion reactions, *Annu. Rev. Sci.* **42**, 447 (1992).
- [9] M. Beckerman, Sub-barrier fusion of two nuclei, *Rep. Prog. Phys.* **51**, 1047 (1988).
- [10] K. Hagino, Sub-barrier fusion reactions, Contribution to the *Handbook of Nuclear Physics*, I. Tanihata, H. Toki and T. Kajino, eds. (Springer, 2022) [arXiv:2201.08061].
- [11] L. A. MacColl, Note on the transmission and reflection of wave packets by potential barriers, *Phys. Rev.* **40**, 621 (1932).
- [12] B. B. Kadomtsev and M. B. Kadomtsev, Wavefunctions of gas atoms, *Phys. Lett. A* **225**, 303 (1997).
- [13] L. C. Vaz, J. M. Alexander, and G. R. Satchler, Fusion barriers, empirical and theoretical: Evidence for dynamics deformation in subbarrier fusion, *Phys. Rep.* **69**, 373 (1981).
- [14] V. V. Dodonov, A. B. Klimov, and V. I. Man'ko, Low energy wave packet tunneling from a parabolic potential well through a high potential barrier, *Phys. Lett. A* **22**, 41 (1996).
- [15] A. V. Dodonov, V. V. Dodonov, Tunneling of slow quantum packets through the high Coulomb barrier, *Phys. Lett. A* **378**, 1071 (2014).
- [16] V. V. Dodonov and A. V. Dodonov, Transmission of correlated Gaussian packets through a delta-potential, *J. Russian Laser Research* **35**, 39 (2014).
- [17] M. A. Andreatta and V. V. Dodonov, Tunneling of narrow Gaussian packets through delta potentials, *J. Phys. A: Math. Theor. Gen.* **37**, 2423 (2004).
- [18] B. C. Lutfuđlu, F. Akdeniz, and O. Bayrak, Scattering, bound, and quasi-bound states of the generalized symmetric Woods-Saxon potential, *J. Math. Phys.* **57**, 032103 (2016).
- [19] A. Arda, O. Aydođdu, and R. Sever, Scattering of the Woods-Saxon potential in the Schroedinger equation *J. Phys. A: Math. Theor.* **43**, 425204 (2010).
- [20] A. Chenu and M. Combescot, Many-body formalism for thermally excited wave packets: A way to connect the quantum regime to the classical regime, *Phys. Rev. A* **95**, 062124 (2017).
- [21] S. Alterman, J. Choi, R. Durst, S. M. Fleming, and W. K. Wootters, The Boltzmann distribution and the quantum-classical correspondence, *J. Phys. A: Math Theor.* **51**, 345301 (2018).
- [22] D. L. Hill and J. A. Wheeler, Nuclear constitution and the interpretation of fission phenomena, *Phys. Rev.* **89**, 1102 (1953).
- [23] C. Eltschka, H. Friedrich, M. J. Moritz, and J. Trost, Tunneling near the base of the barrier, *Phys. Rev. A* **58**, 856 (1998).